Textures and Microstructures, 1991, Vols 14–18, pp. 1159–1164
Reprints available from the publisher
Photocopying permitted by license only

STRUCTURAL CHARACTERIZATION AND TEXTURE ANALYSIS OF Zn-0,15 wt% Pb -0,06 wt% Cd CALOTS FOR DRY CELLS.

F. Cruz[1]; M. Tanus[1]; J. Tobisch[2]; R. Penelle[3]

(1) Laboratorio de Estructura. Facultad de Física-IMRE.
Universidad de La Habana. San Lázaro y L. Habana 4 10400 Cuba.
(2) WB Metall-und-Röntgenphysik Technische Universität.
Dresden 8027 Dresden DDR Mommsenstraße 13.
(3) Laboratoire de Metallurgie Structurale, Bât 413. UA CNRS 1107
Université Paris-Sud, 91405 Orsay Cedex France.

INTRODUCTION

The purpose of this work was to study the role of different parameters: chemical composition and texture on zinc plasticity deformed by inverse extrusion by impact. These zinc calots alloyed with lead and cadmium are used for the production of the negative electrodes of dry cell batteries. We have studied calots of different producers (Japanese, Belgian, Peruvian and Cuban) in particular Cuban calots inclined to crack during the extrusion.
The temperature for the inverse extrusion is approximately 230°C.
The pole figure reported for zinc /1//2/ show a maximum at the centre of the (0002) pole figure measured at the surface of the samples and two maxima approximately tilted by 20° from the normal direction to rolling direction if the measurement is performed on bulk sample.
The chemical composition for these alloys is according to standard Hitachi-Maxwell IS-02-301-1 Pb 0.15 ∓ 0.05 wt% , Cd 0.06 ∓ 0.02 wt% , Cu max 0.005 wt% , Fe max 0.01 wt%
The cadmium is completely dissolved in the zinc matrix for these concentration but lead is immiscible in zinc /3/.
To compare calots of different producers we have done, chemical composition analyses, metallographic studies (including grain size, distribution of compounds, etc), texture analyses, and hardness measurements.

MATERIALS AND METHODS

The calots have the following dimension

Type	Diameter(mm)	Thickness(mm)
R20	30.6	3.1
R14	23.0	3.1

We only know the thermomechanical history for the Cuban sample, in this case the alloy was prepared from pure Zn,Cd, and Pb in a gas furnace without any movement of the melt, afterwards the sheets were cold rolled in one step with a reduction amount of 50%. Samples were named
J (or Japanese) for Japanese sample type R20
P (or Peruvian) for Peruvian sample type R20
B (or Belgian) for Belgian sample type R20
C_1 (or Cuban) for Cuban sample type R14 taken from the top of the melt in the furnace vessel.
C_2 for Cuban sample type R14 taken from the middle of the melt in the furnace vessel.
C_3 for Cuban sample type R14 taken from the bottom of the melt in the furnace vessel.
For metallographic and chemical analysis we used optical scanning electron microscopy and atomic absorption. For texture analysis we measured incomplete pole figures by X-ray diffraction at the surfaces and in the center /4/, complete pole figures were obtained by neutron diffraction, and the texture gradient through the sheet thickness were analyzed by a modifie Harris method using X-ray diffraction/5//6/; thinning was performed by electropolishing.

RESULTS AND DISCUSSION

Chemical analysis: In table 1 we can see the principal elements that were analyzed, other elements such as

$$Ge < 5\times10^{-3}wt\%,\ Co < 1\times10^{-4}wt\%,\ Ni < 1\times10^{-4}wt\%,\ Sn < 1\times10^{-3}wt\%$$
$$Sb < 5\times10^{-4}wt\%,\ As < 1\times10^{-3}wt\%,\ Cu < 2\times10^{-4}wt\%$$

were analyseet too.

Table 1. Chemical Analysis

Sample	Pb(wt%)	Cd(wt%)	Fe(wt%)
C_3	0.35	0.07	0.005
C_2	0.25	0.06	<0.005
C_1	0.21	0.06	<0.005
B	0.18	0.07	<0.005
P	0.19	0.055	<0.005
J	0.19	0.08	<0.005

For these results we can see,that first C_3 and C_2 are outside of the Hitachi-Maxwell standard, and secondly the great influence of the content of lead versus the depth of melt bath of the furnace without movement.

Metallographic analysis: In Fig 1 to Fig 3 we can see the most important details from metallographic analysis of the samples, viz. :

1)The presence of equiaxial grains characteristic of a recrystallized structure (Fig 1,2), and the presence of twinning.
2)In Fig 1 and Fig 2 we can see particles forming chains. Composition of theses particles determined by the microanalysis contain mainly lead, they form like cells with little particles for the Belgian, Peruvian, and Japanese samples, but for Cuban the cells are not defined very well and the particles are bigger.

In one sample without deformation obtained directly from the melt theses chains have the geometry of the isothermal lines during the cooling, whereas no particles are to be found at grain boundaries, we think that they appear in these grain boundary directly from melt, after deformation the process of recrystallization is so rapid that when the first ingot is analyzed we study already a recrystallized material.

Fig 3 shows one side of the crack, we can see a great amount of lead particles. That means that the bad distribution of lead may be the origin of crack, in a similar way as it was for brass.

The size of the zinc grains is very similar in all samples and is roughly 35μm.

Texture analysis: In Fig 4 and Fig 5 we present some results concerning texture, we do not present figures for the Peruvian sample because they are very similar to those of the Japanese one. Table 2 sums up the main results, the most important details from this results are:

a)The values of $\tilde{f}(g)$ are maximal for the Japanese sample and decrease from Japanese -> Peruvian -> Belgian to Cuban.
b)The surface textured is very similar for all the samples, it is like an axial texture of the type $(0,0,0,1)[u,v,t,0]$; when the amount of deformation increases two secondary maxima appear at $\Phi=90,\varphi_2=30$ and $\Phi=90,\varphi_2=0$, which correspond to the ideal components $(0,1,\bar{1},0)[2\bar{v},v,v,w]$ and $(\bar{1},2,\bar{1},0)[u,0,\bar{u},w]$.

The Fig 5a and Fig 5b, shows $f(g)$ and $\tilde{f}(g)$ modeling for the component $(0,0,0,1)[1,0,\bar{1},0]$ at the surface of the Japanese surface using the programs of Matthies /7/. There are secondary maxima at $\Phi=90,\varphi_2=30$ and $\Phi=90,\varphi_2=0$,which are ghost maxima, one could think that the maxima in the Japanese sample are then ghost, but the principal problem is that its intensity is higher than it would correspond to a ghost.

c)By the neutron experiments the texture is found to be similar to that of the surfaces but less sharp, this means that the texture in the center of the sample is lighter ,in Fig 6 we have pole figures messured by neutron . Another interesting aspect is that we obtain the secondary maximum in (0002) pole figure in the transverse direction, which is not the one reported in the literature for zinc/2/.
d)The results of the measurements of inverse pole figures vs the sheet thickness when they are thin appear in Fig 7 , here we have very high values for R(0002) near the surface and at the sixth of the sheet thickness the surface where these values are appreciable, this is approximately 1/3 of the total volume of the sample.

Table 2 Ideal Position

Sample	φ_1	Φ	φ_2	Ideal component	max $\tilde{f}(g)$
Japanese	0-90	0	0-90	(0,0,0,1)[u,v,t,0]	
surface	0	0	0	(0,0,0,1)[1,0,$\bar{1}$,0]	34
	0-90	90	30	(0,1,$\bar{1}$,0)[$2\bar{v}$,v,v,w]	
	90	90	30	(0,1,$\bar{1}$,0)[0,0,0,1]	9
	32	90	30	(0,1,$\bar{1}$,0)[2,$\bar{1}$,$\bar{1}$,1]	7
	0-90	90	0	($\bar{1}$,2,$\bar{1}$,0)[u,0,$\bar{u}$,w]	
	0	90	0	($\bar{1}$,2,$\bar{1}$,0)[1,0,$\bar{1}$,0]	6
	61	90	0	($\bar{1}$,2,$\bar{1}$,0)[3,0,$\bar{3}$,5]	6
Peruvian	0-90	0	0-90	(0,0,0,1)[u,v,t,0]	
surface	0	0	0	(0,0,0,1)[1,0,$\bar{1}$,0]	31
	0-45	90	30	(0,1,$\bar{1}$,0)[2,$\bar{1}$,$\bar{1}$,0]	7
				(0,1,$\bar{1}$,0)[2,$\bar{1}$,$\bar{1}$,1]	
	0	90	0	($\bar{1}$,2,$\bar{1}$,0)[1,0,$\bar{1}$,0]	6
Belgian	0-90	0	0-90	(0,0,0,1)[u,v,t,0]	
surface	14	0	0	(0,0,0,1)[4,$\bar{1}$,$\bar{3}$,0]	23
	0	90	30	(0,1,$\bar{1}$,0)[2,$\bar{1}$,$\bar{1}$,0]	10
Cuban	0-90	0	0-90	(0,0,0,1)[u,v,t,0]	
surface	30	0	0	(0,0,0,1)[2,$\bar{1}$,$\bar{1}$,0]	22
Belgian	0-90	0	0-90	(0,0,0,1)[u,v,t,0]	
neutron	0	0	0	(0,0,0,1)[1,0,$\bar{1}$,0]	5
	0	90	30	(0,1,$\bar{1}$,0)[2,$\bar{1}$,$\bar{1}$,0]	2
Cuban neutron	0-90	0	0-90	(0,0,0,1)[u,v,t,0]	3

Hardness: The results of the measurement of hardness for all the samples are very similar and roughly 32 Hv.

CONCLUSION

1) We have characterized the metallographic structure of calots using for dry cells production, especialy the role that the chains of lead particles play in the occurrence of crack during the extrusion process.

2) We have studied the texture of these materials obtaining that in the surfaces the principal components of texture are (0,0,0,1)[u,v,t,0], (0,$\bar{1}$,$\bar{1}$,0)[$2\bar{v}$,v,v,w], and ($\bar{1}$,2,$\bar{1}$,0)[u,0,$\bar{u}$,w] . The magnitude of the maximum that corresponds to these two last components is related with the degree of deformation. The center of the calots present recrystallized grains of large size which induces a weak texture. The texture of the surfaces is approximately 1/3 of the total volume of the sample and is, of course, not negligible.

REFERENCES
/1/Wassermann G; Grewen J;
Texturen Metallischer Werkstoffe, Springer-Verlag 1962
/2/Philippe M, J; Esling C; Hocheid B;
Texture and Microstructures 1988, vol 7, pp 265-301
/3/Hansen M;
Constitution of Binary Alloys, Ed McGraw-Hill 1959
/4/Bunge H.-J.;
Texture Analysis in Material Science (Mathematical Methods)
Ed Butterworths 1982
/5/Barret C; Massalki T,B;
Structure of Metals, Ed Mc Graw-Hill 3 Ed
/6/Fuentes L; Cruz F; Serra A; Garcia J;
Rev Sociedad Cubana de Física vol XI # 2 , 1989
/7/Matthies S; Vinel G.W; Helming K;
Standard Distributions in Texture Analysis
Ed Academic-Verlag Berlin 1987

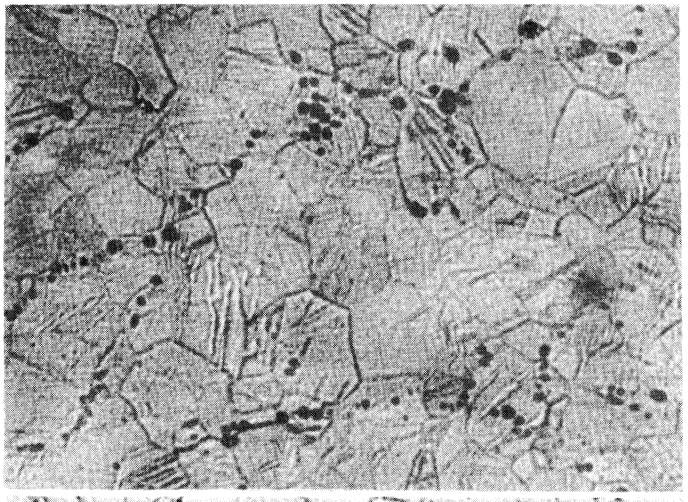

Fig 1
Cuban sample
x 190

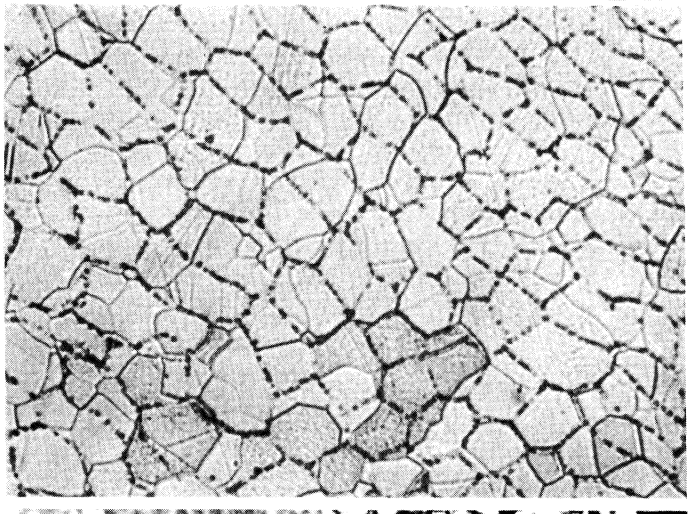

Fig 2
Belgian sample
x 190

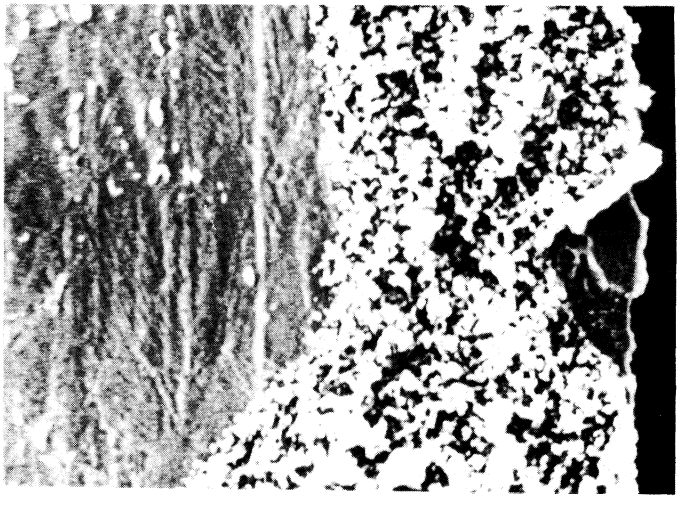

Fig 3
Crack edge
x 330

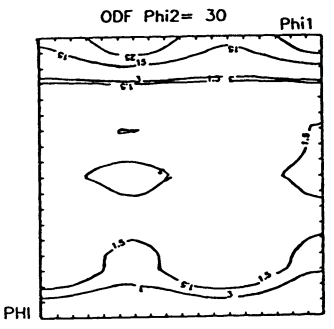

Fig 4
Japanese Surfaces

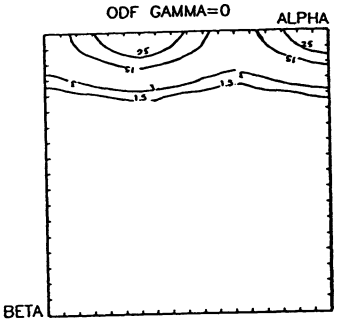

Fig 5a
Modeling f(g)

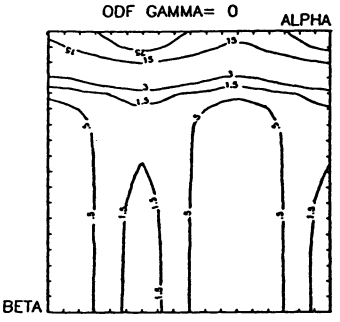

Fig 5b
Modeling f(g)

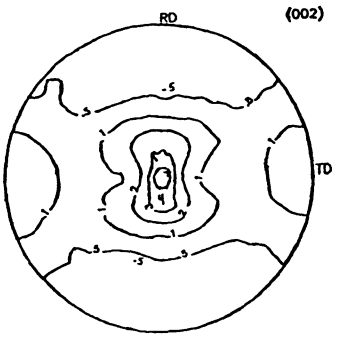

Fig 6a
Belgian
by neutron

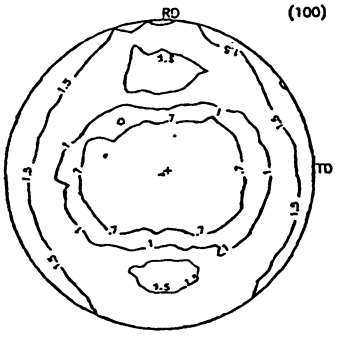

Fig 6b
Belgian
by neutron

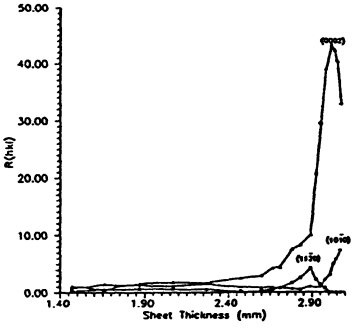

Fig 7 Pole density in the IPF
vs thickness for Belgian sample